

Topography of Cell–Glass Apposition Revealed by Total Internal Reflection Fluorescence of Volume Markers

DAVID GINGELL, IAN TODD, and JULIET BAILEY

Department of Anatomy and Biology as Applied to Medicine, Middlesex Hospital Medical School, London, W1P 6DB, United Kingdom

ABSTRACT We have developed a new method based on total internal reflection fluorescence to map the shape of the region between glass and the lower surface of a living cell spread upon it. Fluorescently labeled nonadsorbing volume marker molecules that cannot penetrate into the cell are locally stimulated so that they fluoresce only very near the glass/medium interface. The total fluorescence intensity at any point beneath the cell depends on the cell-to-glass separation. Focal contacts appear as dark areas owing to dye exclusion, whereas when the gap exceeds ~150 nm, fluorescence asymptotes to the bright background level.

Our technique provides greater contrast than does interference reflection microscopy and is free from errors due to cytoplasmic thickness and refractive index inhomogeneities arising from cytoplasmic inclusions. We have shown that sufficiently large molecules suffer steric exclusion from regions accessible to small molecules, which gives new information about lateral penetrability in the apposition region.

Although the method of total internal reflection fluorescence (TIRF)¹ has been known for almost 20 years (see reference list in reference 1), it has only recently been used to examine cells spread on glass (1). A collimated pencil of light from an argon ion laser is directed through a glass block and is totally internally reflected at the glass/medium interface, as shown in Fig. 1. No light is transmitted, but an inhomogeneous electromagnetic disturbance, the evanescent wave, is generated. This travels parallel to the interface in the aqueous medium but is exponentially damped in a direction perpendicular to the interface. The depth of penetration of the wave into the aqueous medium, which is typically in the range 40–200 nm, is determined by the incident angle and the refractive index step across the interface. This wave can stimulate fluorescence from suitable dyes situated sufficiently close to the interface and has thus been used by Axelrod (1) in conjunction with membrane-associated dyes to obtain images of the lower cell surface.

The novelty of our method involves labeling not the cell surface but the bulk liquid between the glass and the cell. This we have done using as volume markers fluorescein, carboxy-tetramethylrhodamine, and fluorescein-labeled dextrans of various molecular weights. A useful feature of the TIRF method is that the penetration of the evanescent wave can be

limited at will; thus it is possible to avoid excitation of fluorescence in the bulk solution on the far side of the cell. Consequently, where development of the evanescent wave is not hindered, a bright background fluorescence is obtained. Where the cell closely apposes the glass and excludes the fluorescent marker, a less bright or even black image is seen, depending on the degree of exclusion.

We have obtained an expression for the squared amplitude of the evanescent wave as a function of liquid depth z normal to the interface, which shows that the electrical energy decays exponentially with z :

$$A_2^2 = \left(\frac{2A_1 n_2 \cos \phi}{F} \right)^2 \sin^2 \left[\tan^{-1} \left(\frac{n_1 F}{n_2 \cos \phi} \right) \right] e^{-4\pi z F / \lambda} \quad \text{Eq. 1}$$

where $F = (n_1^2 \sin^2 \phi - n_2^2)^{1/2}$, λ is the vacuum wavelength, ϕ is the angle of incidence at the glass/medium interface, measured in the glass (ϕ exceeds the critical angle), n_1 is the refractive index of the glass and n_2 is that of the aqueous phase, A_1 is the amplitude of the incident wave for the p-state of polarization with the electric vector of the plane-polarized laser beam parallel to the plane of incidence, i.e., when the coverslip bearing the cells is horizontal and the plane of vibration of the laser beam is vertical. From Eq. 1 the characteristic decay depth \bar{z} at which the evanescent wave energy has fallen to $1/e$ of its value at the interface is

$$\bar{z} = \lambda \left\{ 4 \pi n_2 \left[\left(\frac{n_1}{n_2} \sin \phi \right)^2 - 1 \right]^{1/2} \right\}^{-2} \quad \text{Eq. 2}$$

¹Abbreviations used in this paper: 4FD and 157FD, fluorescein-labeled dextrans of molecular weight 4,000 and 157,000, respectively; IRM, interference reflection microscopy; TIRF, total internal reflection fluorescence.

For a microscope cover glass with $n_1 = 1.539$ and $n_2 = 1.341$ at $\lambda = 488 \text{ nm}$ we found that $\bar{z} = 60 \text{ nm}$ when $\phi = 75.3^\circ$. This is the condition under which we made our observations.

MATERIALS AND METHODS

Light from a Lexel 85-1 argon ion laser (Lambda Photometrics Ltd., Harpenden, Hertfordshire, U.K.) was passed through a Physik Instrumente spatial filter (Lambda Photometrics Ltd.) and the divergent Gaussian output beam was focused on the specimen by use of a 3-in focal length biconvex lens. A system of mirrors (Melles Griot Ltd., Aldershot, Surrey, U.K.) on Physik Instrumente micrometer adjustable mounts made it possible to define the mean angle of incidence of the collimated beam (2° divergence at the specimen) with a reproducibility of 0.1° . The uncertainty in the penetration depth of the evanescent wave is limited by the divergence to $\pm 1.0 \text{ nm}$. Fig. 1 shows a glass coverslip (c) with adherent cells (b) optically coupled with immersion oil to a glass baseplate (d) attached to an x - y movement (f). The baseplate moves on a film of laser grade siloxane/polyether oil (R. P. Cargille Laboratories, Inc., Cedar Grove, NJ) over a larger fixed glass block (e). Baseplate, oil, and block have similar refractive indices. This arrangement makes it possible to move the field of view without disturbing the laser beam. Cells were viewed with a Zeiss $\times 63$ water immersion objective (a) with a numerical aperture of 1.2. For fluorescence observations Schott OG series colored glass absorption edge filters (H. V. Skan Ltd., Solihull, Warwickshire, U.K.) were used to block laser light scattered in the specimen. For exciting fluorescein we used the 488 nm laser line in conjunction with an OG515 absorption filter; rhodamine was excited at 514.5 nm and an OG550 barrier filter was used. We used a Zeiss UEM microscope (Carl Zeiss Ltd., Welwyn Garden City, Hertfordshire, U.K.) fitted with an epi-illumination system for simultaneous interference reflection microscopy (IRM). This provided surprisingly good interference images with the field stopped well down, despite reduced contrast due to the additional reflection at the objective/water interface. With this microscope it is possible to focus without vertical translation of the stage; this is necessary to keep the laser beam on the specimen area. Quantitative fluorescence measurements were made with an EMI 9863A/100 photon counting photomultiplier (EMI Electronics Ltd., Ruislip, Middlesex, U.K.) with a preamplifier and associated Brookdeal 5C1 photon counter (EG & G Ltd., Bracknell, Berkshire, U.K.) interfaced to a Hewlett-Packard 9845 desktop computer. We took photographs on Ilford XP1-400 film (Ilford Ltd., Basildon, Essex, U.K.) using a chopper in the laser beam, which gave a duty cycle of 0.2 s on and 0.8 s off to allow for recovery after photobleaching of the fluorochrome. The optical equipment was supported on an air table. Fluorescein-labeled dextrans were obtained from Sigma Ltd. (Southampton, Hampshire, U.K.)

Chick heart explants from 7-d-old embryos were cultured on 22-mm square glass coverslips (Chance Brothers Ltd., Warley, Worcestershire, U.K.) for 24–48 h. During this time radial migration of cells from the explant occurs. Actively moving cells furthest from the center we refer to as peripheral, and those that have migrated less far and are static we call inner cells. In some experiments disaggregated limb bud cells were used: cell suspensions were allowed to settle onto coverslips in the presence of the fluorescent volume marker after which we cultured them for 24 or 48 h without removing the marker. For examination of unlabeled cultures by TIRF, the culture medium was carefully replaced with several drops of medium containing fluorochrome solution.

RESULTS

Cells that had been allowed to settle and spread before exposure to fluorescein-labeled dextran of molecular weight 4,000 (4FD) at a final concentration of 10 mg/ml showed extensive dye penetration into the contact zone. The discrete focal contacts of inner stationary cells seen by IRM excluded dye and appeared densely black under TIRF (Fig. 2). Peripheral motile cells sometimes had distinguishable focal contacts under IRM but they more often showed diffuse and wide-spread contacts, as found by Couchman and Rees (2). The paired photographs in Fig. 3, *g*, *h*, and *j*, *k* illustrate peripheral cells in 4FD under TIRF and IRM. Although there is a striking general correspondence between the two types of image, not all densely black contacts visible under TIRF can be traced to unambiguous focal contacts in the IRM images. This is particularly evident upon comparison of Fig. 3 *j* with *k*.

When we repeated these observations with free fluorescein

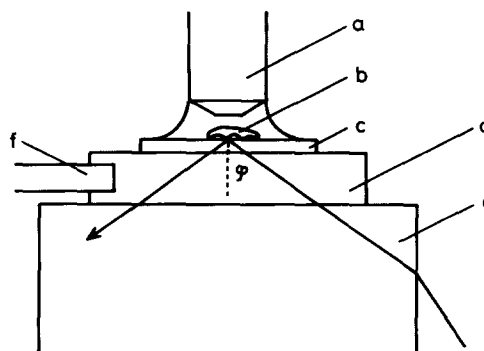


FIGURE 1 Diagram of TIRF method. (a) Objective; (b) cell; (c) coverslip; (d and e) glass blocks; (f) x - y movement. ϕ , angle of incidence of laser beam.



FIGURE 2 Nonmotile inner cell of chick heart explant in the presence of 4FD. The marker is excluded from focal contacts. \bar{z} as in Fig. 3. $\times 1,200$.

and also with carboxytetramethylrhodamine we obtained the same results as with 4FD. However, under laser illumination in the presence of free fluorochromes the images soon lost contrast owing to dye permeation into the cells. Observation and photometric measurement during steady and pulsed illumination indicated photobleaching of fluorescein. The effect was seen as a suffused darkening at the center of each cell image. This brightened after interruption of the laser light for less than a second as fresh dye diffused beneath the cell.

Cells that were allowed to spread and were then exposed to fluorescein labeled dextran of molecular weight 157,000 (157FD) at 10 mg/ml for 0–6 h at 37°C showed a very marked difference between inner and peripheral cells. TIRF images

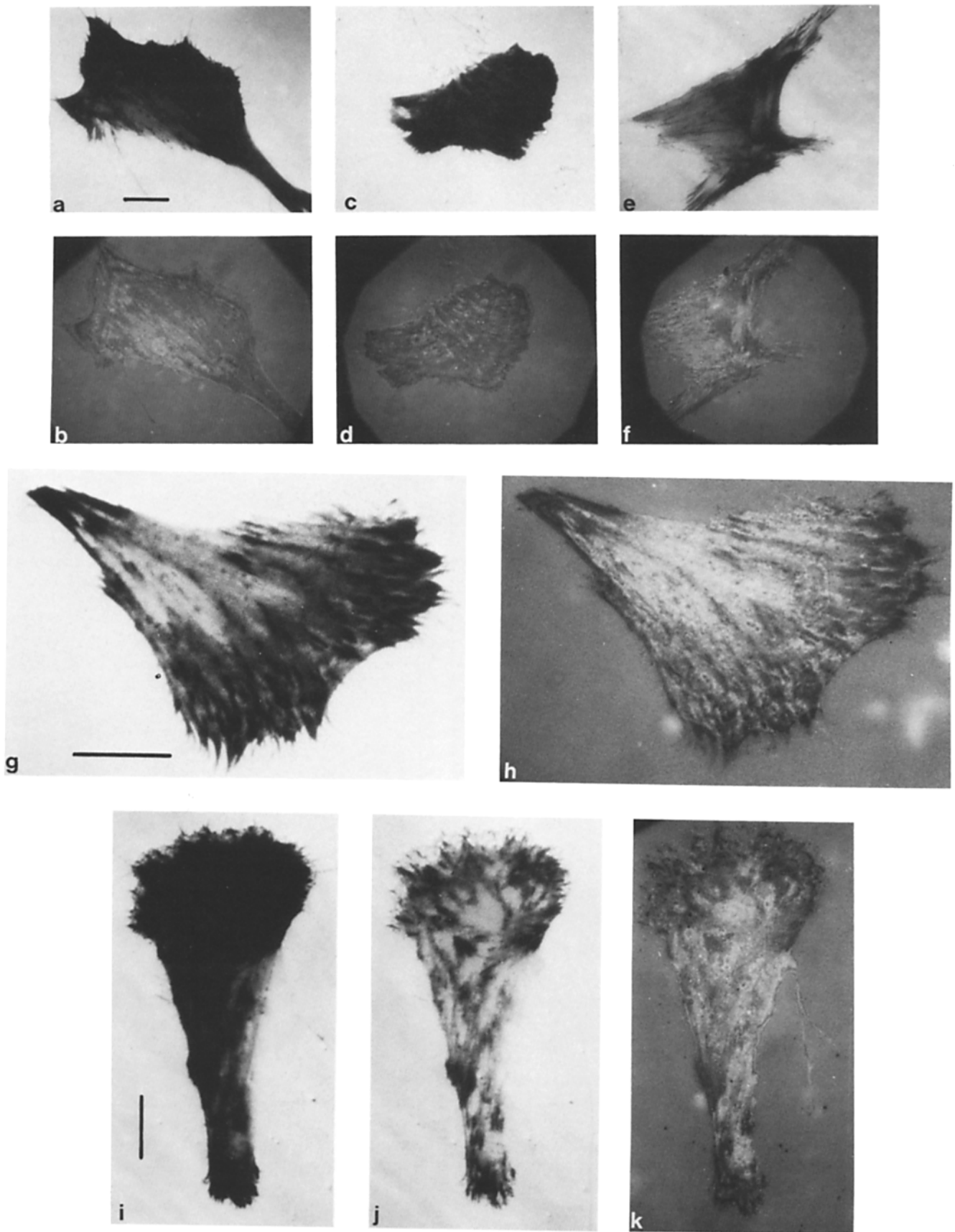


FIGURE 3 Chick heart explant cells. (a, c, and e) Peripheral cells in the presence of 157FD under TIRF; severely limited diffusion of marker beneath cells gives dark images. (b, d, and f) Same cells under interference reflection; discrete focal contacts are not distinguishable. (g) Cell in presence of 4FD under TIRF. (h) Same cell under interference reflection: comparison of the images shows that marker is excluded from focal contacts. (i) Cell in presence of 157FD under TIRF. (j) Same cell in presence of 4FD under TIRF. (k) Same cell under interference reflection. Comparison of *i-k* shows that 157FD is excluded from contact areas accessible to 4FD but the latter is also excluded from intimate (focal?) contacts. (*a-f*) $\times 800$; (*g* and *h*) $\times 1,800$; (*j* and *k*) $\times 1,200$. Bar, $10 \mu\text{m}$ in all micrographs. All cells show evidence of retraction at the leading edge which begins soon after transfer from 37°C to the microscope at 20°C . Incident angle ϕ , 75.3° ; evanescent wave penetration depth \bar{z} , 60 nm in all photographs. Illuminating numerical aperture for interference reflection, 1.05.

of the former were similar in 4FD and 157FD, but many of the peripheral cells appeared densely black in 157FD (Fig. 3, *a* and *c*). Some cells showed a patchwork of black and lighter areas in which filamentous contacts were sometimes seen (Fig. 3*e*). When the 157FD was replaced with 4FD (both at concentrations giving the same TIRF background fluorescence) the images of the dark outer cells were seen to have lightened, and details of their contacts became clearly visible under TIRF (compare Fig. 3, *i* and *j*) while remaining indistinct under IRM (Fig. 3*k*).

Most limb bud cells that had settled and spread in the presence of 157FD for 24 or 48 h gave black images with little or no detectable fluorescence, which showed that the marker had been excluded from the contact zones during spreading and subsequent locomotion. When this was repeated with 4FD (giving the same TIRF background intensity) discrete contacts were visible.

DISCUSSION

The fact that images of peripheral explant cells exposed to label after spreading are much darker in 157FD than 4FD shows that high molecular weight dextran cannot easily penetrate into the apposition zone. This is presumably due to steric exclusion of high molecular weight dextran by cell surface macromolecules or secreted matrix components adsorbed on glass. We can be quite sure that simple diffusion is not the rate limiting factor. This is clear from the observation that after settling and culturing of cells in the presence of 157FD for 24 h the label is largely excluded from the apposition zone. Indeed, the fact that simple unhindered diffusion is several orders of magnitude too fast to account for our results can be shown by calculating diffusion times. If the cell is modeled as a 5- μm -radius disc separated from the glass by a gap much smaller than the cell radius (so that only radial diffusion need be considered) it can be shown, taking hemoglobin as an example (68,000 mol wt; diffusion constant at limiting low concentration $D = 6 \times 10^{-7} \text{ cm}^2/\text{s}$ [3]), that centripetal diffusion would give a concentration at the center equal to 80% of that in bulk within 0.07 s. Even if the diffusion constant of 157FD is 100 times smaller than that of hemoglobin, the time increases to only 7 s. Since diffusion is thus relatively fast there must be an additional steric barrier to diffusion of 157FD. Consequently, we conclude that the penetration of large and small dextrans can be used as differential probes of steric exclusion in the apposition zone.

The fact that molecules as small as fluorescein are limited in their ability to penetrate laterally from the extracellular space into focal contacts indicates that such adhesions have a rather condensed molecular structure with limited free volume for diffusion. It is instructive to compare this conclusion with the results of attempts to label such contacts with specific antibodies from the extracellular medium. Grinnell (4) reported that antibodies to substratum-adsorbed fibronectin could not penetrate into focal contacts, even after permeabilization of the cell. Neyfahk et al. (5) recently described the visualization of focal contacts by means of fluorescence using a variant of Grinnell's antibody exclusion test. Their method involves coating a surface with adsorbed serum protein, letting cells spread on it, then treating with an antibody to an 80,000-mol-wt component of the serum. This is visualized by the sandwich technique, involving two further antibodies, the final one being labeled with fluorescein. After unbound label is washed out the focal contacts are seen to exclude antibody,

giving black patches. Although this interesting method gives information about the distribution of focal contacts, it has disadvantages. The most serious is that the cells are killed by the procedure so that it cannot be used to follow the changing pattern of contacts during locomotion. Furthermore, the method can be used only on antigenic substrata and cannot give cell-to-substratum separation distances. It is complicated and destructive. It is not clear why Triton permeabilization is needed for the second and third antibodies to gain access to any part of the cell contact zone while the first can apparently diffuse in freely (no photograph of this is shown). Indeed Neyfahk et al. stated that the first antibody can diffuse into the focal contacts of living cells. This is surprising in view of our results, but it must be emphasized that we cannot say that none of the volume marker molecules penetrate into focal contacts, only that they are highly excluded.

The technique of labeling an antigenic substratum has recently been extended by Wright and Silverstein (6), who investigated the ability of antibodies to diffuse beneath living macrophages spread on a layer of IgM or IgM mixed with IgG (Fc region pointing towards the cells). They found that fluoresceinated anti-IgM could diffuse beneath cells on a surface of IgM but could not do so when the Fc receptors of macrophages were engaged with IgG on the mixed IgG/IgM surface: even Fab fragments (50,000 mol wt) could not do so. The authors conclude that on surfaces that stimulate a phagocytic response a close seal is formed between the edges of the cells and the substratum. It would be instructive to check these conclusions using TIRF and to see whether small volume marker molecules can penetrate the postulated seal.

It is also interesting that a very dark band seen under interference reflection optics around the edges of some cells, which looks like a more or less continuous region of focal contact, is shown by the corresponding bright TIRF image to be no such thing. It is evidently generated by a band of peripheral cytoplasm where the cell has thinned down to $\approx 100 \text{ nm}$, giving a dark interference image, as Gingell suggested (7).

The volume marker method gives information strictly about the locally available volume per unit image area for fluorochrome penetration beneath cells. If cell surface macromolecules projecting beyond the lipid bilayer into the aqueous gap, or any adsorbed on the glass, do not significantly exclude small marker molecules (such as fluorescein or a low molecular weight dextran conjugate), the TIRF image provides information about the thickness of the cell-to-substratum gap. It gives a map of the topography of the apposition zone, since image irradiance will be quantitatively related to plasma membrane-substratum separation. Work is in progress to test this assumption.

The TIRF bulk volume marker method has significant advantages over IRM, which is currently the most widely used method of observing cell-to-substratum contacts: (*a*) It can be made almost independent of cell thickness by suitable minimization of evanescent wave penetration. (*b*) It is relatively insensitive to cell refractive index and in particular to local cytoplasmic heterogeneity associated with intracellular organelles which cause granularity in IRM images, even at a high illuminating numerical aperture where the effect is minimized. Our TIRF images show clear details of contact that are hard to interpret by interference. (*c*) It gives an image of high contrast, free from glare caused by stray light in the optical system, which can be troublesome in IRM. The excellent contrast is due to the exponential decay of the evanescent

wave (Eq. 1); this emphasizes proximity at the expense of more distant separations, which very rapidly assume background radiance. The radiance ratio (brightest image areas/focal contacts) in the volume marker TIRF method is ~ 10 (probably limited by scattering in the object) as compared with ~ 2 for IRM at high illuminating numerical aperture under optimal conditions, when conventional IRM with an oil immersion objective and an illuminating numerical aperture of 1.18 are used. Thus, TIRF has a fivefold advantage in overall contrast.

It might be thought that the information on cell-to-glass separation that we have obtained with the bulk volume TIRF method could also be obtained by labeling of the cell surface membrane with a fluorescent lipid analogue, antibody, or lectin and assessing the intensity of fluorescence as a function of the penetration depth \bar{z} of the evanescent wave. This is in fact what we had originally intended to do, but the present method is superior for the following reasons: (a) A nonadsorbing inert label that cannot get into the cell is unlikely to perturb it whereas an adsorbing label may well do so. (b) Some labels such as the carbocyanine lipid analogue DiI used by Axelrod (1) stain some cells very unevenly or not at all. (c) Whereas Fab fragments could be used, complete antibody causes more or less marked patching owing to receptor cross linking. (d) For measurement of the separation distance by use of a membrane-adsorbed label it would be necessary to measure both the area density of membrane-associated fluo-

rochrome molecules and also fluorescence efficiency near the lipid bilayer.

It is a pleasure to thank Professor Oliver Heavens for advice on theoretical optics and assistance in deriving Equation 1 and Professor Peter Garland for his unstintingly given advice on setting up the equipment.

D. G. Gingell acknowledges financial support from the Science and Engineering Research Council.

This work is dedicated to the memory of David Ubee, whose energy and expertise will be greatly missed.

Received for publication 3 December 1984.

REFERENCES

1. Axelrod, D. 1981. Cell-substrate contacts illuminated by total internal reflection fluorescence. *J. Cell Biol.* 89:141-145.
2. Couchman, J. R., and D. A. Rees. 1979. The behavior of fibroblasts migrating from chick heart explants: changes in adhesion, locomotion and growth, and in the distribution of actomyosin and fibronectin. *J. Cell Sci.* 39:149-165.
3. Riveros-Moreno, V., and J. B. Wittenberg. 1972. The self diffusion coefficients of myoglobin and hemoglobin in concentrated solutions. *J. Biol. Chem.* 247:895-901.
4. Grinnell, F. 1980. Visualization of cell-substratum adhesion plaques by antibody exclusion. *Cell Biol. Int. Rep.* 4:1031-1036.
5. Neyfakh, A. A., I. S. Tint, T. M. Svitkina, A. D. Bershadsky, and V. I. Gelfand. 1983. Visualization of cellular focal contacts using a monoclonal antibody to 80kD serum protein adsorbed on the substratum. *Exp. Cell Res.* 149:387-396.
6. Wright, S. D., and S. C. Silverstein. 1984. Phagocytosing macrophages exclude proteins from the zones of contact with opsonized targets. *Nature (Lond.)* 309:359-361.
7. Gingell, D. 1981. The interpretation of interference reflection images of spread cells: significant contributions from this peripheral cytoplasm. *J. Cell Sci.* 49:237-247.